Age of the Batoka basalts, northern Zimbabwe, and the duration of Karoo Large Igneous Province magmatism

D. L. Jones

Department of Physics, University of Zimbabwe, Harare, Zimbabwe

R. A. Duncan

College of Oceanic and Atmospheric Sciences, Oregon State University, Corvallis, Oregon (rduncan@oce.orst.edu)

J. C. Briden

Environmental Change Institute, University of Oxford, Oxford, England, United Kingdom (Jim.Briden@eci.ox.ac.uk)

D. E. Randall

British Antarctic Survey, High Cross, Madingley Road, Cambridge, England, United Kingdom
Department of Earth Sciences, University of Oxford, Oxford, England, United Kingdom

Now at Environment Agency, Manley House, Exeter, England, United Kingdom

C. MacNiocaill

Department of Earth Sciences, University of Oxford, Oxford, England, United Kingdom

[1] **Abstract:** Analysis of the Batoka Basalts exposed in the Zambezi Gorge some 40 km east of Victoria Falls characterizes them as high Fe, moderately high Ti, and low K, P, and Zr tholeiites. The ^{40}Ar-^{39}Ar age determinations are tightly clustered at 180–179 Ma. All of the lavas that were sampled have normal paleomagnetic polarity, and the corresponding pole position is 63.9°N, 260.6°E, A_{95} = 14.9°. In South Africa, Lesotho, and Namibia the vast majority of Karoo basalts were extruded at 183 ± 1 Ma with some as young as 179 Ma [*Duncan et al.*, 1997]. Paleomagnetic and geochemical correlation of the ~179 Ma rocks between Zimbabwe and Lebombo supports the conclusion that the age difference is real and hence confirms the estimate of ~5 Myr for the duration of emplacement of the Karoo Large Igneous Province.
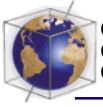
1. Introduction

[2] Remnants of the Karoo Large Igneous Province (LIP) are found throughout southern Africa over a vast area stretching from the Cape Peninsula in South Africa to the Zambezi Valley in northern Zimbabwe and southern Zambia (Figure 1). This Mesozoic continental flood basalt event was thought at one time, on the basis of K-Ar data and the extent of the magmatism, to span a time interval of ~50 Myr [*Fitch and Miller*, 1984]. Recently, however, an extensive ^{40}Ar-^{39}Ar study of the lavas from Lesotho, Namibia, and South Africa has shown that the vast majority of the basalts were extruded at 183 ± 1 Ma, with a total age range of $184-179$ Ma [*Duncan et al.*, 1997]. In an allied study, *Hargraves et al.* [1997], working with over 2000 paleomagnetic samples from 691 sites in Karoo igneous rocks, have shown that the Lesotho remnant records a single reversal with the upper two thirds of the pile having normal polarity. The upper one third of the Lebombo sequence contains evidence of at least one more reversal, while the age data suggest that this section is slightly younger than the Lesotho pile (but still within the $184-179$ Ma range). A third study by *Marsh et al.* [1997] shows that geochemistry may be used for stratigraphic correlation purposes between the various South African and Lesotho remnants. In particular, the Lesotho basalts are characterized by low-TiO_2 (~1 weight percent) content, while the upper parts of the Springbok Flats sequence and parts of the Lebombo remnant consist of high-TiO_2 (~3 weight percent) lavas.

[3] Only a sparse amount of geological or geophysical work has been done on the Karoo volcanics of northwest Zimbabwe. *Nairn* [1960] reported paleomagnetic results from three flows near Victoria Falls and one sample from near Bulawayo. Normal polarity was observed in the 12 samples that gave acceptable results. No demagnetization of samples was done, and the results are regarded as preliminary at best. *Cox et al.* [1965] report geochemical analyses of five basalt samples from the Victoria Falls area, and they showed a mean TiO_2 content of nearly 3 weight percent. Extensive geological work has been done on the Karoo volcanics of southeast Zimbabwe by *Cox et al.* [1965], who report analyses showing a somewhat lower average TiO_2 content (~2.5 weight percent). *Brock* [1968] gives preliminary paleomagnetic results from four sites from the lower part of the Mwenezi lava sequence. He reported poor response during demagnetization, but the indications were that all sites were reversely magnetized.

[4] Geotechnical investigations into a possible hydroelectric scheme on the Zambezi River at Batoka Gorge ~40 km east of Victoria Falls have provided an opportunity to study the lavas at that site (17.90° S, 26.17°E) by providing access to a 250 m exposed section and fresh borecore material. The purpose of the project was to establish precisely the age of the Batoka lavas relative to those elsewhere in southern Africa. The wider significance of this information is that it improves our knowledge of the extent and duration of magma emplacement in this LIP.

2. Geology and Sampling

[5] The Batoka basalts are a succession of lava flows that form a flat plateau into which deep gorges with steep sides have been incised by the Zambezi River and its tributaries. Geotechnical investigations at the Batoka Gorge dam site [*Chaplow et al.*, 1984] revealed 13 near-horizontal lava flows varying in thickness from 10 to 80 m. Seven of the flows are below riverbed level, and flows 8–13 outcrop. Lack of sedimentary horizons between flows suggests eruption over a short time interval. The lava flows were subjected to subaerial weath-
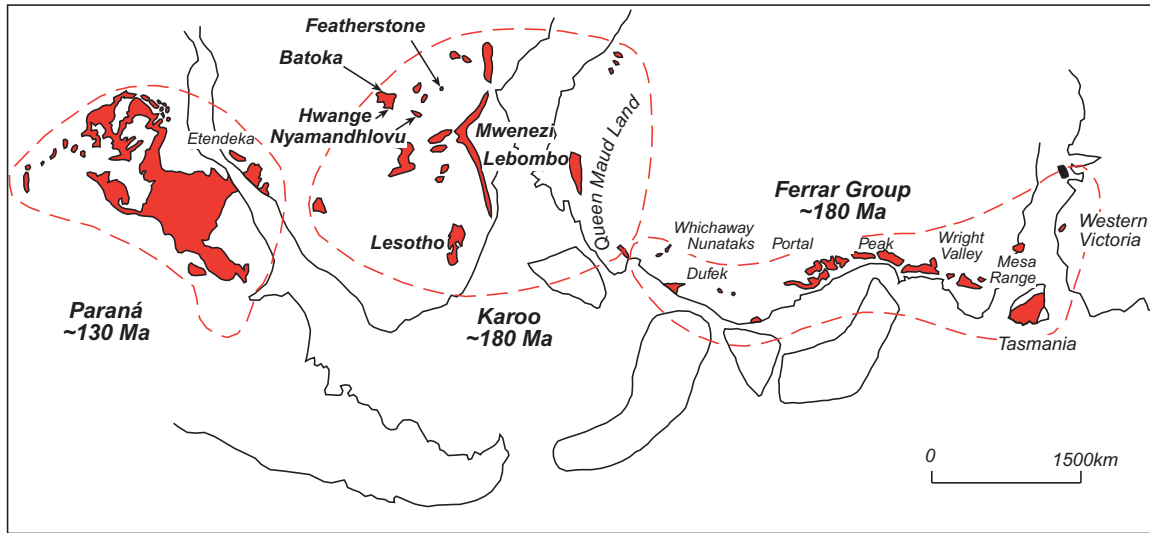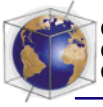
Figure 1. Sketch map of Gondwana illustrating the location of Mesozoic continental flood basalts. Southern African localities mentioned in the text are named: Hwange and Mwenezi were formerly Wankie and Nuanetsi, respectively. The paleopositions of the tectonic elements of west Antarctica are shown schematically (modified from *Hergt et al.* [1991]).

ering on extrusion and then, following shallow burial, low-temperature hydrothermal alteration. These processes have produced layering within each flow with fresh massive interiors and brecciated flow tops.

[6] There is a rough track, which leads from the plateau down through the lava flows to the river, some 250 m below. In situ outcrop is

limited, but it was possible to drill samples at five sites (BA1–BA5) in the massive interiors of four of the flows for paleomagnetic studies (Table 1). From four to six samples were drilled at each site and labeled; for example, BA5.1 is the first sample from site 5. Samples were oriented by means of Sun compass or, occasionally, owing to the deep, narrow nature of the cleft down which the track runs, by mag-

Table 1. Paleomagnetic Results From Surface Sites Sampled in Batoka Gorge[a]

| Site | Flow | n | Paleomagnetic Direction | | | | VGP | |
			Dec	Inc	k	α_{95}	Latitude, °N	Longitude, °E
BA1	8	8	339.2	−57.9	88.5	5.9	62.5	243.2
BA2	9	3	357.1	−43.4	24.8	25.3	82.1	225.7
BA3	11	6	336.3	−61.1	106.5	6.5	58.4	240.9
BA4	13	6	324.0	−42.3	374.5	3.5	55.9	278.8
BA5	13	8	321.1	−39.8	170.9	4.2	53.3	282.1
Mean			335.0	−49.7	33.9	13.3		

[a] Notation is as follows: n is the number of specimens included in the site mean; Dec (Inc) is declination (inclination) of paleomagnetic direction; k and α_{95} are precision parameter and 95% confidence limits on direction following *Fisher* [1953]; VGP is site virtual geomagnetic pole. The samples all come from a 1 km traverse at 17.90°S, 26.17°E.
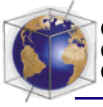
netic compass. The geotechnical work involved the drilling of many oriented boreholes, and the core has been stored in sheds at the top of the gorge. Two samples, A and B, generally >10 cm in length, were obtained from each of six borecores (BH403, BH404, and BH405 in flow 8; BH51 and BH52 in flow 9; BH53 in flow 11). Although the borehole samples are not fully oriented, their dip is known. Given that the inclination of the magnetic field in Karoo times was steep, measurements on specimens drilled from the borecores can give information on magnetic polarity. Further, the borecore pieces provided fresh material for geochronology and geochemistry.

3. Paleomagnetic Methods and Analysis

[7] Paleomagnetic analysis of standard 2.5 cm cylindrical specimens (one or two from each drilled sample) was carried out at the paleomagnetic laboratories in Oxford University and the University of Zimbabwe. Specimen natural remanent magnetizations (NRM) were measured using a Molspin MS2 or, in a few cases, a two-axis CCL cryogenic magnetometer. Specimen magnetizations were investigated through progressive stepwise demagnetization using thermal or two-axis tumbling alternating field (AF) methods. Results from pilot specimens from each of the surface sites revealed that both demagnetization methods provided satisfactory isolation of magnetic components, and AF treatment was used for the remainder of the study. At AF demagnetization levels above ~25 mT, samples showed the effects of rotational remanent magnetization (RRM). To minimize the effects of RRM, each specimen was demagnetized and measured twice at each treatment stage, with the sample inverted in the demagnetizer for the second run. The mean of the two measurements was then taken as the result for the demagnetization step [*Hillhouse*, 1977]. RRM became domi-

nant above ~70 mT and precluded further treatment.

[8] After correction for the RRM the demagnetization behavior of specimens was displayed on vector-end-point diagrams (Figure 2) and stereographic projections, and principal component analysis of the data was performed using the IAPD computer program [*Torsvik*, 1986]. Magnetic components were defined by a minimum of three demagnetization steps and were considered stable when they had a maximum angular deviation not exceeding 10°. Mean directions for each surface sampling site and for the formation were calculated by combining directions using *Fisher* [1953] statistics (Table 1).

4. Magnetic Mineralogy

[9] The magnetic mineralogy of representative specimens from the surface sites was investigated through isothermal remanent magnetization (IRM) acquisition experiments, where magnetic fields of up to ~820 mT were applied to the specimens using a Molspin pulse magnetizer. Additionally, high-temperature susceptibility behavior was examined for some specimens. Examples of the results obtained are shown in Figure 3.

[10] During IRM acquisition, all specimens show a rapid rise in magnetization with increased applied field, with saturation being achieved after application of a field in the range 80–200 mT. Following saturation, specimens were subjected to progressively increasing reverse fields in order to determine their coercivities of remanence ($(Bo)_{CR}$). Values of $(Bo)_{CR}$ lie in the range 7–26 mT with most lying around 20–26 mT. Together, the data are consistent with a magnetite or titanomagnetite carrier [*Thompson and Oldfield*, 1986]. The low remanence coercivity observed in some experiments suggests that the magnetite may be Ti-rich or that some grains are pseudosingle
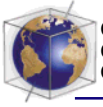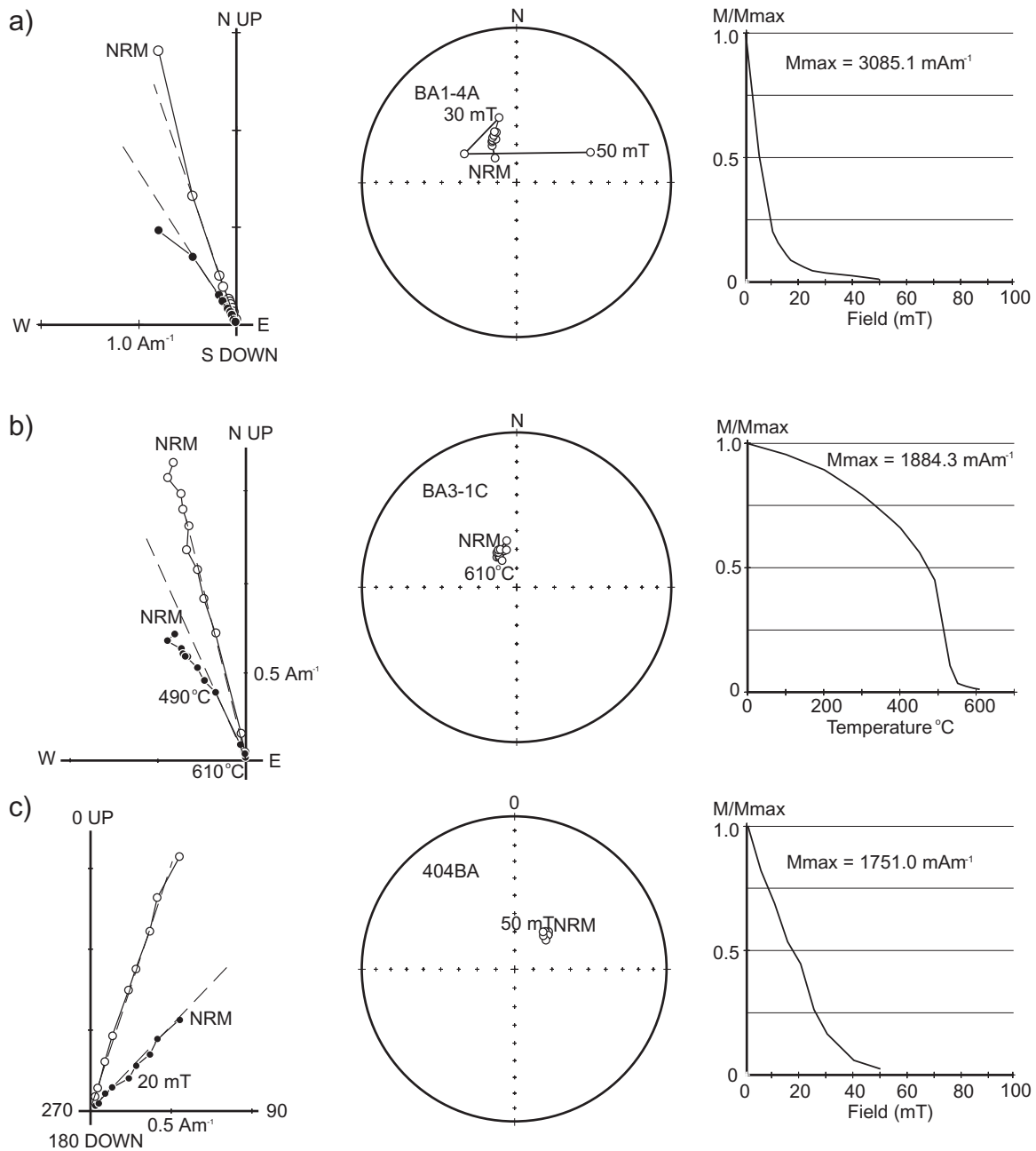
Figure 2. Representative orthogonal and equal area projections of demagnetization data for the Karoo basalts. Figures 2a and 2b are from surface samples, Figure 2c is from a bore core, and the declination is unconstrained and expressed relative to an arbitrary fiducial direction mark on the sample. In orthogonal plots, open (solid) symbols represent vertical (horizontal) projections. On stereoplots, open (solid) circles represent negative (positive) inclinations. Normalized decay curves of the magnetization reveal the coercivity and unblocking spectra observed.
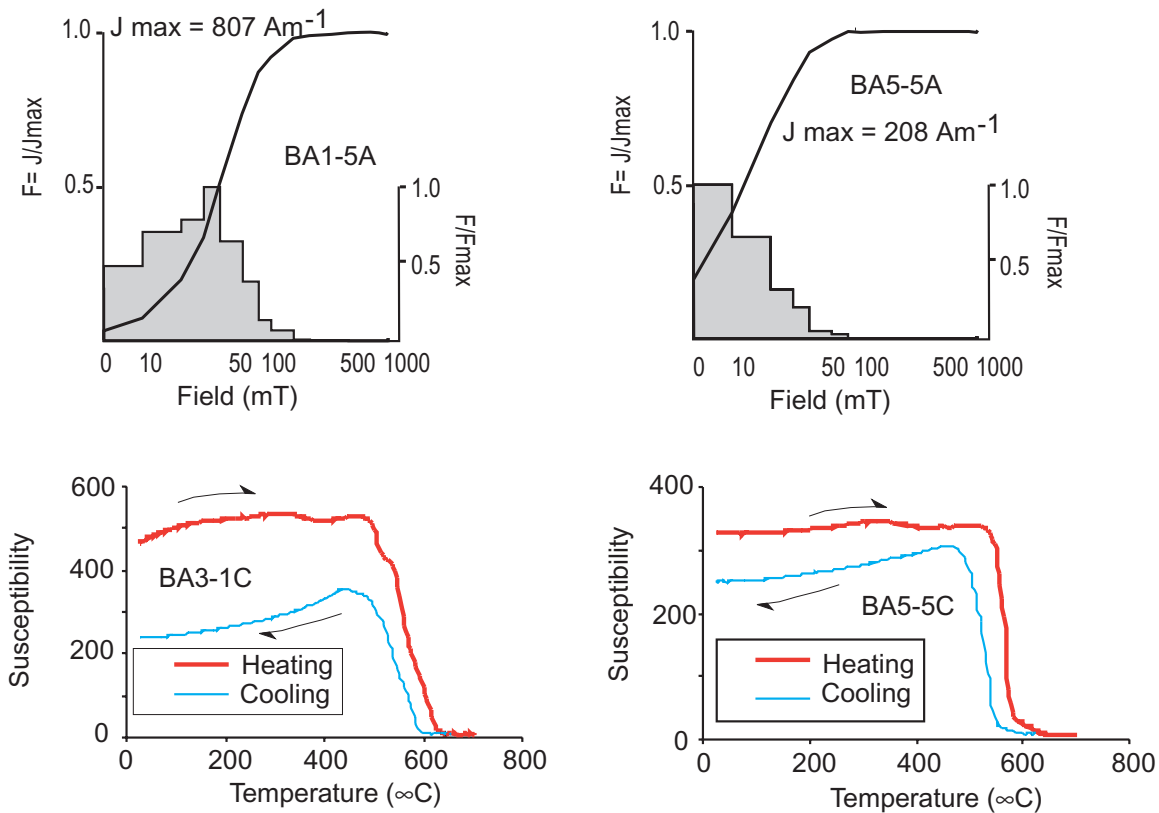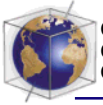
Figure 3. Isothermal remanent magnetization (IRM) acquisition and high-temperature susceptibility curves for representative specimens. For IRM acquisition, applied fields were progressively applied up to a maximum of 820 mT. The bar chart shows rate of change in acquired magnetization. For high-temperature susceptibility curves, powdered specimens were heated to 700°C and then cooled.

domain to multidomain in size in these specimens.

[11] Results from the high-temperature susceptibility studies support the information gained from the IRM work but demonstrate that heating causes alteration. On heating, there is a small rise in the susceptibility, and then a fall over approximately the 250°–450°C temperature range, probably owing to the presence of titanomagnetite. There is a subsequent rapid decrease in susceptibility around 580°C with a small "tail" that extends up to ∼610°C (Figure 3). In some samples, notably those with lower coercivities, this tail is much larger, and the Curie temperatures are between 580°C and

610°C (Figure 3). Although not visible in Figure 3, the data also show a rise in susceptibility from ∼670°C. During cooling, there is no evidence of the titanomagnetite peak observed in the heating run. Partial heating and cooling runs with progressively increased maximum temperatures reveal that the alteration occurs dominantly around 300°–450°C and 550°–620°C. The interpretation of the data is that on heating, the titanomagnetite exsolves into a titanium-rich component and Ti-poor magnetite, some of which then oxidizes to maghemite that eventually inverts to hematite. On cooling, the absolute susceptibility is reduced as a consequence of the lower susceptibility of the newly formed hematite. The

altered distribution of titanium in the remaining titanomagnetite-magnetite phase leads to a smearing of the Curie temperatures (Figure 3).

[12] The high-temperature susceptibility studies, in conjunction with the IRM acquisition studies, suggest that magnetite with some associated titanomagnetite is the dominant magnetic carrier of both the induced and natural remanence.

5. Paleomagnetic Results

5.1. Samples From Surface Sites

[13] Specimen behavior during demagnetization is consistent, and a characteristic remanence (ChRM) was recovered from all five sites. NRM intensities range from 0.36 to 5.56 A m^{-1}, with most lying around 2–3 A m^{-1}, and are consistent within individual sites. Specimens display simple demagnetization behavior, whereby a single, origin-bound, linear component of magnetization is readily isolated after removal of a low-coercivity component by AF treatment to about 2–10 mT (Figure 2a). During thermal treatment a low-unblocking temperature component is removed by 100°C, and an intermediate component, with a direction close to that of the ChRM, is removed by ~480–500°C (Figure 2b). In most cases the low coercivity and unblocking temperature components are poorly grouped directionally, both within and between sites.

[14] These components are interpreted as viscous remanent magnetizations (VRM) probably acquired during storage and/or during laboratory processing. The intermediate component observed during the thermal demagnetization is probably a result of overlap in the blocking spectra of the ChRM and the low temperature VRM components.

[15] All of the five sites from the surface flows carry a consistent direction, and the ChRM

direction is in the northwest quadrant with negative inclination, indicating that all sites have normal polarity (Table 1; Figure 4). One site, BA2, has a small number of specimens contributing to the mean and hence a large 95% confidence limit. This was due to the limited amount of unweathered material available at the site. Despite the low number of specimens in this site, the magnetic behavior observed is the same as, and the mean directions are consistent with, data from the other sites. It is therefore included in the mean calculation and the remainder of the analysis. The demagnetization results and those from the rock magnetic studies are consistent with the hypothesis that the ChRM is of primary origin. A paleomagnetic pole calculated from the site virtual geomagnetic poles lies at 63.9°N and 260.6°E (K = 27.4; A_{95} = 14.9°).

5.2. Bore Core Samples

[16] Bore core pieces were cut to produce plane ends perpendicular to the core axis, and standard 2.5 cm diameter samples were drilled out along the bore core axes. Paleomagnetic measurements thus determine inclination of remanance relative to the bore core axis.

[17] A specimen from each of the bore cores pieces was demagnetized using AF treatment. The samples were fresher in appearance than the surface samples but yielded near identical demagnetization behavior: a single component of magnetization recovered after removal of a randomly oriented VRM by treatment to, at most, 25 mT and generally to 10 mT (Figure 2c).

[18] Three of the boreholes (BH403, BH404, and BH405) were drilled only 2° off vertical, and the inclination of the ChRM should thus reflect the inclination of the ancient magnetizing field. All samples from these boreholes are from flow 8, and measured inclinations group fairly closely around a simple arithmetic mean
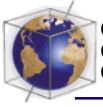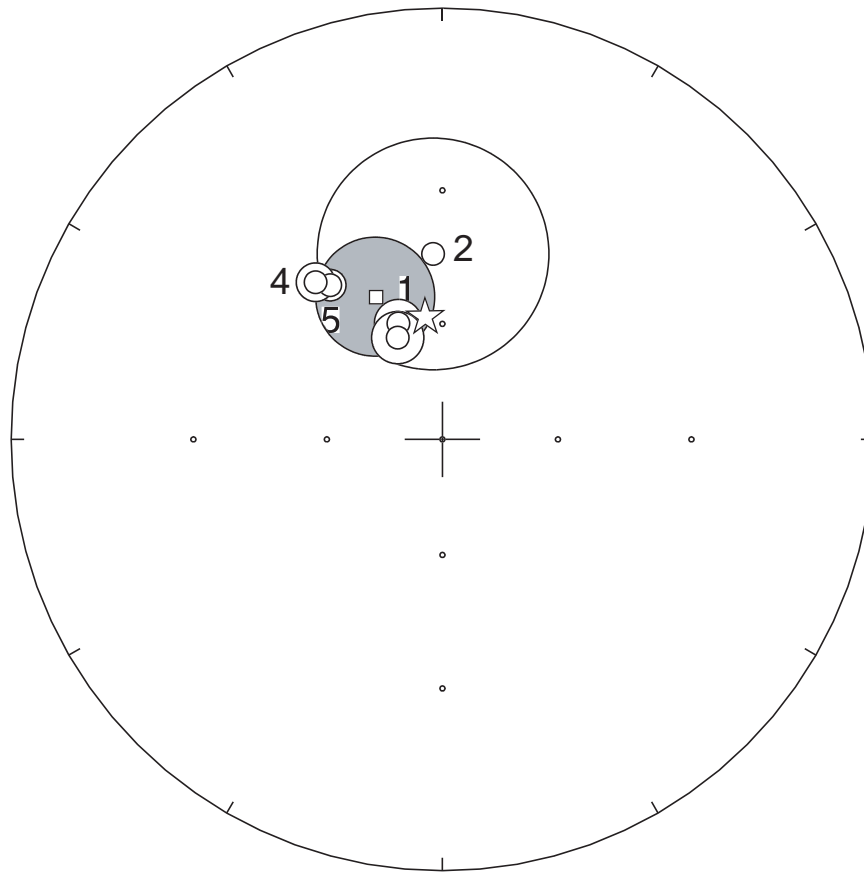
Figure 4. Site mean directions of characteristic remanence. Open (solid) circles represent negative (positive) inclinations with associated 95% confidence limits. The formation mean direction is represented by a square, and its 95% confidence limit is shaded. The direction of the present Earth's magnetic field is indicated by a star.

of −55°. This compares well with the mean inclination measured at surface site BA1 of −58°. Samples from borehole BH52, also near vertical, record a lower (mean) inclination of −35° for flow 9 compared to −43° recorded from surface site BA2. Of the two inclined boreholes, BH53 (from flow 11) matches the surface data very closely, but BH51 (from flow 9) does not. However, there are inconsistencies in the data from core BH51, both within a core piece and between core pieces, and the results are therefore not considered further.

[19] All of the recovered bore core pieces were from flows sampled at the surface, and thus they do not add to our knowledge of the polarity pattern in the deeper part of the Batoka lava pile; they do, however, confirm the validity of the surface site results.

6. The ^{40}Ar-^{39}Ar Geochronology

[20] Unheated cores from outcrops and bore cores were processed for age determinations. Minor oxidized rinds were sawn off, and then

Table 2. The ^{40}Ar-^{39}Ar Incremental Heating Ages for Batoka Basalts, Zimbabwe[a]

Sample Number (Depth in Borecore, m)	Material	Total Fusion Age, Ma	Plateau Age (±2σ, Ma)	^{39}Ar (Percent of Total)	Isochron Age (±2σ, Ma)	N	^{40}Ar/^{36}Ar Intercept ± 2σ	J
BH403B (268.0)	whole rock	177.5	(179.7 ± 0.9)	60.7	(179.8 ± 2.3)	6	292 ± 8	0.001496
BH404A (258.4)	plagioclase	185.3	(179.8 ± 1.2)	73.0	(180.1 ± 1.6)	5	296 ± 12	0.001685
BH404A (258.4)	whole rock	186.4	no plateau (recoil)	no isochron				0.001440
BH405B (246.8)	plagioclase	180.6	(179.2 ± 0.9)	85.0	(180.5 ± 2.8)	8	297 ± 27	0.001673
BH52A (5.0)	whole rock	196.2	181.3 ± 1.5	30.1	182.1 ± 5.3	5	473 ± 72	0.001596
BH53A (59.1)	whole rock	182.5	no plateau (recoil)	no isochron				0.001549
BA1.5	whole rock	188.9	no plateau (recoil)	no isochron				0.001375
BA3.6	whole rock	179.9	no plateau (recoil)	no isochron				0.001433
BA5.5	whole rock	179.2	no plateau (recoil)	no isochron				0.001494

[a]Ages are reported relative to biotite monitor FCT-3 (28.04 ± 0.12 Ma), which is calibrated against hornblende Mmhb-1 (523.5 Ma [Renne et al., 1994]). Plateau ages are the mean of concordant step ages (N is the number of steps) weighted by the inverse of their variances. Calculations use the following decay and reactor interference constants: $\lambda_e = 0.581 \times 10^{-10}$ yr^{-1}, $\lambda_\beta = 4.963 \times 10^{-10}$ yr^{-1}, $(^{36}Ar/^{37}Ar)_{Ca} = 0.000264$, $(^{39}Ar/^{37}Ar)_{Ca} = 0.000673$, and $(^{40}Ar/^{39}Ar)_{Ca} = 0.01$. J is the neutron fluence factor, determined from measured monitor ^{40}Ar/^{39}Ar. Preferred ages are shown in parentheses and are discussed in the text.

the samples were crushed and sieved to retain the 0.1–0.5 mm size fraction. Samples are sparsely plagioclase-phyric to aphyric, generally fine-grained, holocrystalline basalts of tholeiitic composition; both whole rocks and plagioclase separates were analyzed. Alteration is present as variable, low-temperature replacement of groundmass by smectitic clays. Phenocrysts and microlites of plagioclase are fresh. The crushed fractions of whole rock were washed in water to remove dust; the plagioclase crystals, separated magnetically and hand-picked, were washed in a sequence of mild HNO$_3$, HCl, and HF to remove any adhering fragments of groundmass, then washed in water in an ultrasound bath. Between 50 and 100 mg of each sample were wrapped in Cu foil and loaded in quartz vials for neutron irradiation.

[21] Samples were irradiated for 6 hours at 1 MW power at the Oregon State University TRIGA reactor. The total fluence of fast neutrons in producing ^{39}Ar from ^{39}K was moni-

tored with biotite standard FCT-3 (28.04 Ma [Renne et al., 1994]). After decay of short-lived radionuclides the samples were loaded in a glass manifold above a low-blank, double-vacuum resistance furnace, where they were dropped one at a time and heated incrementally to investigate the isotopic composition of Ar released with increasing temperature, measured with an MAP 215/50 mass spectrometer. Further details of the experimental procedure are described by Duncan et al. [1997].

[22] Results of the ^{40}Ar-^{39}Ar experiments are presented in Table 2 and Figure 5. Age determinations were calculated in three ways. First, age spectra (step ages versus temperature, represented by %^{39}Ar released) were examined for evidence of concordant step ages for a majority of the samples' Ar (called a plateau). In three samples (BH404A and BH405B plagioclase, and BH403B whole rock), good plateaus were apparent, defining a narrow age range from 179 to 180 Ma, while in a fourth (BH52A) a two-step plateau comprising only 30% of the total
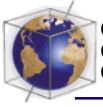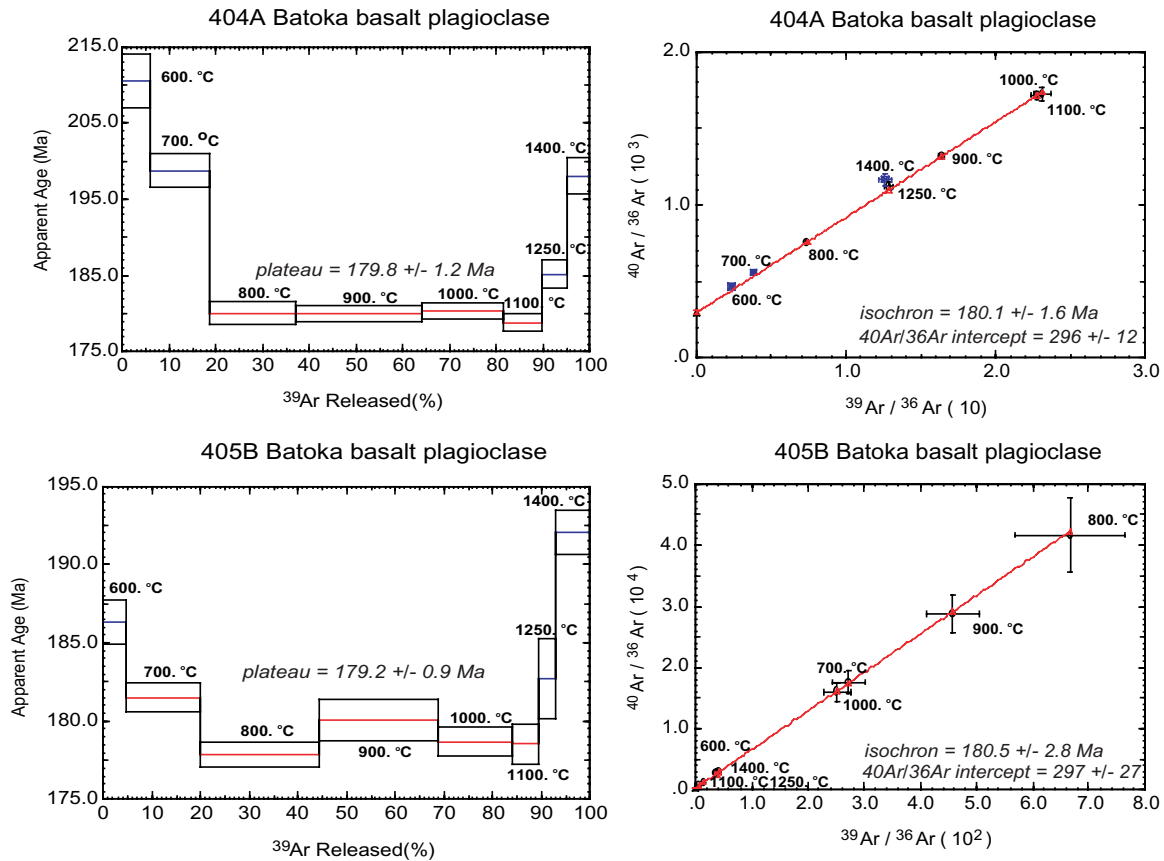
Figure 5. Representative age spectra and isochron plots for Batoka basalt age determinations. Plateau ages are weighted means of concordant, sequential step ages. Isochron ages are calculated from the best fit slope of step compositions. The $^{40}Ar/^{36}Ar$ intercept is the initial composition of Ar in the sample at crystallization (atmosphere is 295.5). All errors are 2 standard deviation.

sample ^{39}Ar produced an age concordant with the reliable plateau ages. In the remaining whole-rock samples, step ages decrease with increasing temperature as a result of irradiation-induced ^{39}Ar and ^{37}Ar recoil from K- and Ca-rich sites within these fine-grained basalts. For these samples the best estimate of crystallization age is the total fusion age, obtained by summing all of the step compositions, as if the sample had been heated to fusion in one step. These total fusion ages range from 178 to 196 Ma and are comparable to conventional K-Ar ages. The third age calculation derives from the correlation of the step Ar compositions ($^{40}Ar/^{36}Ar$

versus $^{39}Ar/^{36}Ar$ isochrons). These correlations allow determination of the initial composition of Ar in the sample at crystallization, assumed to be atmospheric ($^{40}Ar/^{36}Ar = 295.5$) in the age spectra calculations. For the three samples that produced plateau ages, the isochrons revealed initial atmospheric compositions, confirming the reliability of the plateau ages. The isochron ages are concordant but have slightly larger fitting uncertainties. The fourth sample (whole rock BH52A) appears to have retained some nonatmospheric Ar at the time of crystallization, which explains its older total fusion age, stemming from erroneous low- and high-tempera-

Geochemistry
Geophysics
Geosystems

G^3

JONES ET AL.: BATOKA BASALTS AND KAROO MAGMATISM

2000GC000110

ture step ages. The isochron age and abbreviated plateau (based on the two most radiogenic steps) appear to be reliable estimates of the crystallization age.

7. Discussion

7.1. Stratigraphic Implications

[23] The tight cluster of reliable ^{40}Ar-^{39}Ar ages at 179–180 Ma falls at the young end of the range of age determinations for the Karoo igneous event (184–179 Ma [Duncan et al.,

1997]) and confirms that the Batoka basalts are northern remnants of this large province that once covered much of southern Africa and large parts of Antarctica. The new ages correspond most closely with the upper part of the Lebombo section (South Africa), where lavas of the Sabie basalt formation are overlain by the Jozini rhyolites. The ~5 Myr duration of activity for the Karoo Igneous Province is comparable with the peak activity for other LIPs (e.g., the North Atlantic Igneous Province, 62–55 Ma [Sinton and Duncan, 1998; Tegner and Duncan, 1999]).

Table 3. XRF Major and Trace Element Compositions of Batoka Basalts[a]

	BH403B	BH52A	BH53A	BH405B	BA1.5	BA3.6	BA2.6	BA5.5	BH404A
Major Elements (wt%)									
SiO_2	51.83	49.72	51.07	50.11	49.51	50.50	51.56	50.24	49.46
Al_2O_3	13.53	13.88	14.39	13.50	13.95	14.09	13.48	14.09	13.20
TiO_2	2.29	2.24	2.51	2.12	2.27	2.54	2.44	2.28	2.00
FeO*	13.24	13.23	12.26	14.50	13.46	12.43	13.31	11.76	15.46
MnO	0.21	0.21	0.18	0.21	0.21	0.19	0.20	0.18	0.21
CaO	9.57	10.45	9.96	9.98	10.23	9.94	8.64	10.88	10.19
MgO	5.37	6.02	5.70	5.96	5.86	5.71	5.64	6.99	6.00
K_2O	0.80	0.57	0.71	0.57	0.74	0.70	0.58	0.30	0.56
Na_2O	2.64	2.34	2.60	2.36	2.49	2.67	2.62	2.21	2.24
P_2O_5	0.26	0.24	0.28	0.23	0.26	0.28	0.26	0.24	0.21
Total	99.73	98.90	99.66	99.53	98.97	99.04	98.74	99.17	99.52
Trace Elements (ppm)									
Ni	66	79	86	72	71	91	85	98	79
Cr	110	140	131	123	117	143	169	176	135
Sc	39	36	34	35	44	32	41	38	37
V	353	382	364	346	374	370	387	354	347
Ba	220	188	216	155	226	217	188	182	171
Rb	14	7	12	7	12	12	11	1	6
Sr	276	285	354	280	280	353	324	378	276
Zr	165	154	179	145	162	179	166	157	137
Y	36	33	36	34	37	35	32	31	33
Nb	10.6	10.0	12.3	8.7	9.9	12.0	10.6	9.8	9.5
Ga	20	24	22	20	26	24	22	22	21
Cu	213	191	239	217	218	205	450	178	217
Zn	111	110	106	123	115	106	112	98	123
Pb	1	0	3	9	2	0	5	0	6
La	9	5	19	13	10	11	6	17	20
Ce	40	42	53	35	36	59	44	49	21
Th	1	0	1	0	4	0	1	1	1

[a]Analyses performed at the GeoAnalytical Laboratory, Washington State University; total Fe expressed as FeO. Details of methods, including standard analyses, are given by Johnson et al. [1999].
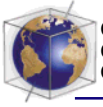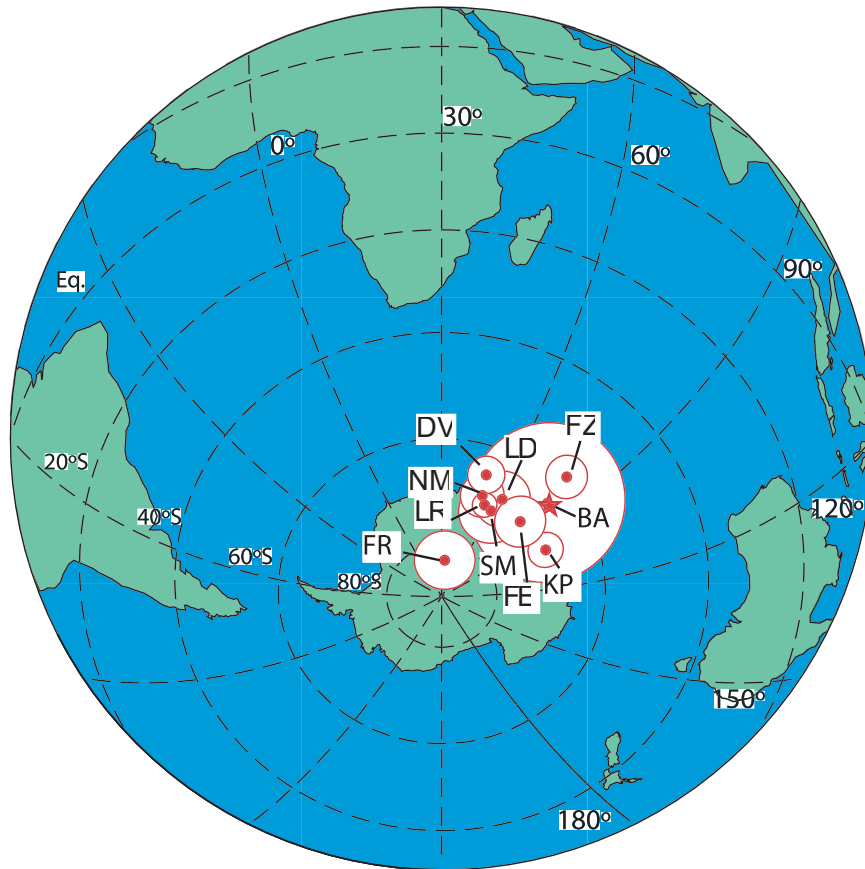
Figure 6. Karoo and West African early Jurassic paleomagnetic south poles [*Hargraves et al.*, 1999] compared with the result from the present study (BA, denoted by a star) and the Ferrar Dolerite pole (FE) rotated into African coordinates [*Hargraves et al.*, 1997] as described in the text. Notation: FR, Freetown Complex, Sierra Leone; FZ, Foum Zguid dyke, Morocco; DV, Draa Valley sills, Morocco; NM, North Mauretania dolerites; SM, South Mauretania dolerites; LD, Liberian dykes; LR, La Reculée sediments; KP, Karoo Igneous Province.

[24] In an effort to more precisely correlate the Batoka basalts with well-described lava sections that occur to the southeast, we determined major and trace element compositions for nine samples (Table 3). These are remarkably uniform and can be characterized as moderately high Ti, low K, P, and Zr, and high Fe tholeiites. They are most similar to the basalts of the Sabie River area, central Lebombo region, described by *Sweeney et al.* [1994], which contain $2-2.5\%$ TiO_2 and $160-210$ ppm Zr and which lie below the Jozini rhyolites. Hence the compositional correlation sup-

ports the age correspondence. Remnants of lava flow sequences closer to the Batoka area, such as Nyamandhlovu, Featherstone, and Hwange, are predominantly higher K, P, and Zr rocks than at Batoka [*Cox et al.*, 1967], although some analyses approach those reported here.

[25] If the Batoka basalts are indeed best correlated with the Sabie River basalts, this could indicate synchronous eruption, perhaps via dyke propagation, over distances up to 800 km. This is a conclusion reached earlier from

comparison of Karoo lavas in Namibia with those found in the Lesotho section [*Marsh et al.*, 1997]. The normal polarity observed in the Batoka basalts is consistent with this suggested correlation. *Brock*'s [1968] preliminary study of the Mwenezi lavas identified a possible reversal. Reversals were also observed high up in the Karoo sequence in the Lebombo section [*Hargraves et al.*, 1997], and it is possible that *Brock* [1968] observed one of these. If this is so, then many, if not all, of the Zimbabwean lavas were emplaced toward the end of Karoo igneous activity.

7.2. Paleomagnetic Pole

[26] A paleomagnetic north pole calculated from the site virtual geomagnetic poles (Table 1) lies at 63.9°N and 260.6°E with the radius of the circle of 95% confidence about the mean pole position (A_{95}) = 14.9°. *Hargraves et al.* [1997], combining results from the Lesotho lavas, Karoo dolerite dykes and sills, Sabie River basalts, Mashikiri and Letaba lavas, and Jozini rhyolites, calculate a paleomagnetic north pole at 69.2°N and 278.3°E with A_{95} = 3.3°. The Batoka pole lies only 8.8° from the highly reliable *Hargraves et al.* [1997] Karoo pole with the latter's circle of confidence lying wholly within that of the Batoka pole. There is thus no statistically significant difference between the two poles, which are shown in Figure 6 as south poles lying southeast of the African continent.

[27] *Duncan et al.* [1997] argue that the Ferrar Group igneous activity in Antarctica and Australia (Figure 1) is virtually synchronous with the Karoo igneous activity. This enabled *Hargraves et al.* [1997] to compare the Ferrar Antarctic pole with their Karoo pole using the *Martin and Hartnady* [1986] reconstruction. They concluded that (p. 203) "the difference [7.3°] between the Antarctic and Karoo poles is within error" (see Figure 6). If the Batoka pole

is combined with the six results of *Hargraves et al.* [1997], a mean pole at 68.4°N and 273.2° E results with A_{95} = 3.1°. Although the angle between this pole and the (rotated) Antarctic pole is marginally smaller at 5.8°, this does not change *Hargraves et al.*'s [1997] conclusion.

8. Conclusions

[28] This study, from the northwest extremity of Karoo igneous activity in southern Africa, confirms that the Batoka basalts were erupted late in the major phase of activity ~180 Myr ago. The correlation of geochemical and paleomagnetic properties in lavas of this age from Zimbabwe and Lebombo lends further strength to the conclusion that these rocks are significantly younger than the acme of Karoo activity at ~183 Ma and hence to the conclusion of *Duncan et al.* [1997] that the Karoo LIP was emplaced over ~5 Myr. Over this longer interval the area covered by lava flows extended at least 1300 km from near Victoria Falls to Lesotho and the southern Lebombo and farther into Queen Maud Land (Figure 1). Taken together with the Ferrar Group igneous activity in Antarctica and Australia (Figure 1), which *Duncan et al.* [1997] argue is virtually synchronous with the Karoo, igneous activity extended at least 6000 km along the Gondwana margin in Early Jurassic time.

Acknowledgments

References

Brock, A., Paleomagnetism of the Nuanetsi igneous province and its bearing upon the sequence of Karoo igneous activity in southern Africa, *J. Geophys. Res.*, *73*, 1389–1397, 1968.

Chaplow, R., C. D. Eldred, and J. S. Sutton, Geotechnical investigations for a hydro-electric scheme on the Zambezi River at Batoka Gorge, Zimbabwe/Zambia, in *Soil Mechanics and Foundation Engineering: Proceedings of the Eighth Regional Conference for Africa, Harare, 1984*, edited by J. R. Boyce, W. R. Mackechnie, and K. Schwartz, pp. 3–12, A. A. Balkema, Brookfield, Vt., 1984.

Cox, K. G., R. L. Johnson, L. J. Monkman, C. J. Stillman, J. R. Vail, and D. S. Wood, The geology of the Nuanetsi igneous province, *Philos. Trans. R. Soc. London, Ser. A*, *257*, 71–218, 1965.

Cox, K. G., R. MacDonald, and G. Hornung, Geochemical and petrological provinces in the Karoo basalts of southern Africa, *Am. Mineral.*, *52*, 1451–1474, 1967.

Duncan, R. A., P. R. Hooper, J. Rehacek, J. G. Marsh, and A. R. Duncan, The timing and duration of the Karoo igneous event, southern Gondwana, *J. Geophys. Res.*, *102*, 18,127–18,138, 1997.

Fisher, R. A., Dispersion on a sphere, *Proc. R. Soc. London, Ser. A*, *217*, 295–305, 1953.

Fitch, F. J., and J. A. Miller, Dating Karoo rocks by conventional K-Ar and ^{40}Ar/^{39}Ar age spectrum methods, *Spec. Publ. Geol. Soc. S. Afr.*, *13*, 247–266, 1984.

Hargraves, R. B., J. Rehacek, and P. R. Hooper, Palaeomagnetism of the Karoo igneous rocks in southern Africa, *S. Afr. J. Geol.*, *100*, 195–212, 1997.

Hargraves, R. B., J. C. Briden, and B. A. Daniels, Palaeomagnetism and magnetic fabric in the Freetown Complex, Sierra Leone, *Geophys. J. Int.*, *136*, 705–713, 1999.

Hergt, J. M., D. W. Peate, and C. J. Hawkesworth, The petrogenesis of Mesozoic Gondwana low-Ti flood basalts, *Earth Planet. Sci. Lett.*, *105*, 134–148, 1991.

Hillhouse, J. W., A method for the removal of rotational remanent magnetization acquired during alternating field demagnetisation, *Geophys. J. R. Astron. Soc.*, *50*, 29–34, 1977.

Johnson, D. M., P. R. Hooper, and R. M. Conrey, XRF analysis of rocks and minerals for major and trace elements on a single low dilution Li-tetraborate fused bead, *Adv. X-Ray Anal.*, *41*, 843–867, 1999.

Marsh, J. S., P. R. Hooper, J. Rehacek, R. A. Duncan, and A. R. Duncan, Stratigraphy and age of Karoo basalts of Lesotho and implications for correlations within the Karoo igneous province, in *Large Igneous Provinces: Continental, Oceanic and Planetary Flood Volcanism, Geophys. Monogr. Ser.*, vol. 100, edited by J. J. Mahoney and M. F. Coffin, pp. 247–272, AGU, Washington, D. C., 1997.

Martin, A. K., and C. J. H. Hartnady, Plate tectonic development of the southwest Indian Ocean: A revised reconstruction of east Antarctica and Africa, *J. Geophys. Res.*, *91*, 4767–4786, 1986.

Nairn, A. E. M., A palaeomagnetic survey of the Karroo System, *Overseas Geol. Miner. Resour.*, *7*, 398–410, 1960.

Renne, P. R., A. L. Deino, R. C. Walter, B. D. Turrin, C. C. Swisher, T. A. Becker, G. H. Curtis, W. D. Sharp, and A.-R. Jaouini, Intercalibration of astronomical and radioisotopic time, *Geology*, *22*, 783–786, 1994.

Sinton, C. W., and R. A. Duncan, ^{40}Ar-^{39}Ar ages of lavas from the southeast Greenland margin, ODP Leg 152, and the Rockall Plateau, DSDP Leg 81, in *Proc. Ocean Drill. Program Sci. Results*, *152*, 387–402, 1998.

Sweeney, R. S., A. R. Duncan, and A. J. Erlank, Geochemistry and petrogenesis of Central Lebombo basalts of the Karoo Igneous Province, *J. Petrol.*, *37*, 95–125, 1994.

Tegner, C., and R. A. Duncan, ^{40}Ar-^{39}Ar chronology for the volcanic history of the southeast Greenland rifted margin, *Proc. Ocean Drill. Program Sci. Results*, *163*, 53–62, 1999.

Thompson, R., and F. Oldfield, *Environmental Magnetism*, 227 pp., Allen and Unwin, Winchester, Mass., 1986.

Torsvik, T. H., *Interactive Analysis of Palaeomagnetic Data: IAPD User Guide*, 74 pp., Univ. of Bergen, Bergen, Norway, 1986.